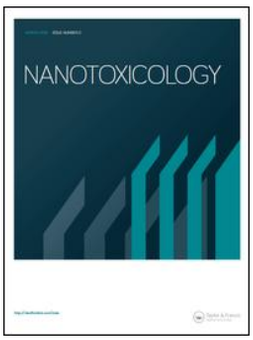

Nanotoxicology

ISSN: 1743-5390 (Print) 1743-5404 (Online) Journal homepage: http://www.tandfonline.com/loi/inan20

Weathering in soil increases nanoparticle CuO bioaccumulation within a terrestrial food chain

Alia D. Servin, Luca Pagano, Hiram Castillo-Michel, Roberto De la Torre-Roche, Joseph Hawthorne, Jose A. Hernandez-Viezcas, René Loredo-Portales, Sanghamitra Majumdar, Jorge Gardea-Torresday, Om Parkash Dhankher & Jason C. White

To cite this article: Alia D. Servin, Luca Pagano, Hiram Castillo-Michel, Roberto De la Torre-Roche, Joseph Hawthorne, Jose A. Hernandez-Viezcas, René Loredo-Portales, Sanghamitra Majumdar, Jorge Gardea-Torresday, Om Parkash Dhankher & Jason C. White (2017) Weathering in soil increases nanoparticle CuO bioaccumulation within a terrestrial food chain, Nanotoxicology, 11:1, 98-111, DOI: 10.1080/17435390.2016.1277274

To link to this article: http://dx.doi.org/10.1080/17435390.2016.1277274

NANOTOXICOLOGY, 2017
VOL. 11, NO. 1, 98–111
http://dx.doi.org/10.1080/17435390.2016.1277274

Taylor & Francis
Taylor & Francis Group

ORIGINAL ARTICLE

Weathering in soil increases nanoparticle CuO bioaccumulation within a terrestrial food chain

Alia D. Servin[a], Luca Pagano[a,b,c], Hiram Castillo-Michel[d], Roberto De la Torre-Roche[a], Joseph Hawthorne[a], Jose A. Hernandez-Viezcas[e], René Loredo-Portales[f,g], Sanghamitra Majumdar[a], Jorge Gardea-Torresday[e,h], Om Parkash Dhankher[b] and Jason C. White[a]

[a]Department of Analytical Chemistry, Connecticut Agricultural Experiment Station, New Haven, CT, USA; [b]Stockbridge School of Agriculture, University of Massachusetts, Amherst, MA, USA; [c]Department of Life Sciences, University of Parma, Parma, Italy; [d]European Synchrotron Radiation Facility, Grenoble Cedex, France; [e]Chemistry Department, University of Texas at El Paso, El Paso, TX, USA; [f]Universidad de Guanajuato Noria Alta s/n 36000, Guanajuato, Mexico; [g]Elettra Sincrotrone Trieste, Basovizza, Italy; [h]University of California Center for Environmental Implications of Nanotechnology (UC CEIN), El Paso, TX, USA

ABSTRACT

This study evaluates the bioaccumulation of unweathered (U) and weathered (W) CuO in NP, bulk and ionic form (0–400 mg/kg) by lettuce exposed for 70 d in soil co-contaminated with field incurred chlordane. To evaluate CuO trophic transfer, leaves were fed to crickets (*Acheta domestica*) for 15 d, followed by insect feeding to lizards (*Anolis carolinensis*). Upon weathering, the root Cu content of the NP treatment increased 214% (327 ± 59.1 mg/kg) over unaged treatment. Cu root content decreased in bulk and ionic treatments from 70–130 mg/kg to 13–26 mg/kg upon aging in soil. Micro X-ray fluorescence (μ-XRF) analysis of W-NP-exposed roots showed a homogenous distribution of Cu (and Ca) in the tissues. Additionally, micro X-ray absorption near-edge (μ-XANES) analysis of W-NP-exposed roots showed near complete transformation of CuO to Cu (I)-sulfur and oxide complexes in the tissues, whereas in unweathered treatment, most root Cu remained as CuO. The expression level of nine genes involved in Cu transport shows that the mechanisms of CuO NPs (and bulk) response/accumulation are different than ionic Cu. The chlordane accumulation by lettuce upon co-exposure to CuO NPs significantly increased upon weathering. Conversely, bulk and ionic exposures decreased pesticide accumulation by plant upon weathering. The Cu cricket fecal content from U-NP-exposed insects was significantly greater than the bulk or ion treatments, suggesting a higher initial NP accumulation followed by significantly greater elimination during depuration. In the lizard, Cu content in the intestine, body and head did not differ as a function of weathering. This study demonstrates that CuO NPs may undergo transformation processes in soil upon weathering that subsequently impact NPs availability in terrestrial food chains.

ARTICLE HISTORY
Received 16 September 2016
Revised 1 December 2016
Accepted 13 December 2016

KEYWORDS
Trophic transfer of CuO NPs; pesticides; synchrotron; CuO nanoparticles; aged/weathered nanoparticles

Introduction

The rapid increase in the use of nanotechnology and engineered nanoparticles (NPs) in sectors as wide-ranging as medicine, electronics, textiles, cosmetics and food packaging (Keller & Lazareva, 2014; Sajid et al., 2015) has raised concerns among the scientific community over possible impacts on environmental and human health. There has also been great interest in the use of nanotechnology in agriculture, with the most common applications being nanofertilizers and nanopesticides to improve crop productivity, efficiency and safety (Servin et al., 2015; Servin & White, 2016). Copper, largely due to its antimicrobial properties, has been among the most widely discussed NPs in agriculture (Hong et al., 2015; Le Van et al., 2016a). In addition, each year approximately 20 million cubic meters of wood are treated with aqueous copper carbonate preservative that is known to contain particles in the nanoscale (~20 nm) (Evans et al., 2008). Current estimates on the consumption of copper-based preservatives for wood protection in North America approach 79,000 tons per year (Anjum et al., 2015). Although these applications clearly have significant benefit for agriculture and related consumer products, the consensus among the scientific community is that our understanding of NP fate and effects in the environment is currently inadequate.

Copper is typically distributed in soil at low concentrations (or at least low availability) and is widely recognized as an essential micronutrient for photosynthetic electron transport, mitochondrial respiration, oxidative stress responses and hormone signaling (Anjum et al., 2015). However, there is concern that the increased use of nano-based Cu products may increase its background concentration in soil (Trujillo-Reyes et al., 2014), which at high enough levels could impact plant growth, development and productivity. For example, Musante & White (2012) reported that Cu NPs at 100 and 500 mg/L reduced zucchini (*Cucurbita pepo*) growth and transpiration volume by 60–70%. Dimkpa et al. (2012) reported reduced wheat growth (*Triticum aestivum*) upon exposure to 500 mg/kg CuO NP in sand, noting that the accumulated Cu was present largely as CuO and Cu (I) sulfur complexes. Kim et al. (2012) reported 50% higher activity of SOD and POD activities in *Cucumis sativus* root cells when exposed at 100 mg/L CuO. Wang

CONTACT Jason C. White Jason.White@ct.gov Department of Analytical Chemistry, The Connecticut Agricultural Experiment Station, 123 Huntington Street, P.O. Box 1106, New Haven, CT 06504-1106, USA

Supplemental data for this article can be accessed here.

et al. (2012) reported that although CuO NPs had no effect on maize (*Zea mays* L.) germination; the fresh weight of seedling's roots and shoots were reduced by 60% and 34%, respectively. Last, Hong et al. (2015) reported that Cu NP at 5–20 mg/L altered the uptake of P, S and Fe in hydroponically grown alfalfa (*Medicago sativa*) and lettuce (*Lactuca sativa*).

Although a robust literature assessing the phytotoxicity of engineered nanomaterials has begun to develop, by necessity much of this work has occurred in model systems/media, often focusing on high dose, single solute exposures over short periods of time. Consequently, drawing conclusions about NP fate and effects in complex soil environments based on this data is highly problematic. Clearly, NPs released to soil could aggregate significantly; changing size, shape and surface chemistry in an unknown fashion over time. The impact of these transformations during weathering on particle bioaccumulation, toxicity, and risk is poorly understood (Servin & White, 2016). In one relevant study, Scheckel et al. (2010) reported the stability of Ag and ZnO NPs in kaolin suspensions during 18 months of aging; the authors reported that Zn^{2+} was rapidly released and complexed but that Ag NP stability largely depended on the presence of other constituents (ions) in the solution. Romero-Freire et al. (2017) investigated the influence of aging for 6 months on the availability and toxicity of Zn NPs and $ZnCl_2$ to earthworms (*Eisenia andrei*) in three soils. The authors reported that in the NP exposure, both soil properties and aging status influenced available Zn in the soil pore water and the Zn content accumulated within earthworm tissues (Romero-Freire et al., 2017). Seitz et al. (2015) aged TiO_2 NPs for 0–6 d and reported increased toxicity to *Daphnia magna* with 1 and 3 d aged particles as compared to 0 d controls. Clearly more investigation into the effects of NP aging and transformation in soil on particle bioaccumulation within terrestrial food chains is needed.

Previous studies have demonstrated NP accumulation and trophic transfer within terrestrial food chains (Judy et al., 2011; Unrine et al., 2012). For example, accumulation of Ce from soil by exposed zucchini plants was significantly greater in the NP form (as compared to bulk) and this greater particle-size dependent contaminant burden was maintained through exposed herbivore and carnivore species; notably, the total amount of Ce (regardless of particle size) did decrease by 10–100 times at each subsequent level of the food chain (Hawthorne et al., 2014). Separately, we evaluated the transfer of La from bulk and NP La_2O_3-exposed lettuce to crickets (*Acheta domestica*) and then to mantises (*Tenodera aridifolia sinensis*) (De la Torre et al., 2015); here, particle size did not significantly impact element accumulation or transfer among species and similar to the previous study, La content decreased significantly at each trophic level. Conversely, Majumdar et al. (2016) reported time-dependent accumulation and biomagnification of Ce within bean beetles (*Epilachna varivestis*) that had consumed kidney bean (*Phaseolus vulgaris*) exposed to bulk or NP CeO_2. In the current study, we evaluate the possible bioaccumulation and transfer of unweathered (U) and weathered (W) CuO NPs and bulk particles, as well as Cu ion, from soil by lettuce (*Lactuca sativa*) to primary consumers (crickets; *A. domestica*) and subsequent secondary consumers (lizards; *Anolis carolinensis*). In addition, the soil that was used was contaminated with field incurred residues of chlordane and DDx (DDT + metabolites); NP exposure is known to impact the bioavailability of co-existing contaminants (De la Torre-Roche et al., 2013a,b) and as such, weathered pesticide uptake by lettuce was evaluated as a function of Cu type and weathering. Last, both Cu distribution and speciation were evaluated in exposed lettuce roots by μ-XRF and μ-XANES, respectively, and the expression of nine genes related to Cu transport was evaluated as a function of exposure type.

Materials and methods

Materials

Copper oxide (CuO) NPs (99% purity, 40 nm particle size) were acquired from US Research Nanomaterials (Houston, TX). NPs in deionized water (DI) were characterized for average particle size, zeta potential and by transmission electron microscopy (TEM) in a parallel study (Pagano et al., 2016). The average hydrodynamic particle diameters (*dh*) and zeta potential (ζ) in DI water were 162.0 nm and −11.5 mV, respectively (Pagano et al., 2016). We do note that the importance of these values is limited since the solutions are added to soil, where particle characteristics will certainly change dramatically prior to and during exposure. Bulk CuO (99.9%) and $CuSO_4{\cdot}5H_2O$ (ion control) were acquired from Sigma-Aldrich (Newburyport, MA) and Strem Chemicals (Newburyport, MA), respectively. The CuO NPs concentration was selected based on previous similar studies in literature (Dimkpa et al., 2012; Perreault et al., 2010). Individual batches of CuO (NP and bulk) solutions were prepared by suspending the commercial nanopowder in DI water to concentrations that would yield 400 mg/kg upon soil amendment. For $CuSO_4{\cdot}5H_2O$, the concentration used was equal to the 10% of the metal content present in NP and bulk material treatments, conservatively assuming 10% particle dissolution (Dimkpa et al., 2013). In order to avoid aggregation, CuO suspensions were ultrasonicated with a probe sonicator (Fisher Scientific, FB-505, Hampton, NH) at 40% amplitude for 2 min.

Soil preparation

Soil containing field incurred chlordane resulting from historical application (Isleyen et al., 2013) was collected from top 50 cm of the Connecticut Agricultural Experiment Station (CAES) in New Haven, CT. The soil is characterized as sandy loam (69% sand; 22% silt; 8.6% clay; 4.3% organic matter; pH 5.9; cation exchange capacity 18.6 cmol/kg). The soil was air-dried, sieved to 2 mm, and stored at room temperature until use. Copper suspensions were added to a mixture of 530 g of soil and 30 g of vermiculite, and were manually mixed in an effort to achieve homogeneity. Half of the soil replicates were prepared as unweathered treatments (seedlings added the same day as Cu amendments) and the remaining replicates were prepared and weathered by maintaining field moisture under ambient temperature and light for 70 d prior adding the seedlings. Hereafter, treatments are referred to as unweathered (U) (prepared same day as planting) and weathered (W) treatments (prepared 70 d prior planting). After 70 days of growth, lettuce plants were harvested and prepared for analysis or supplied to crickets as described below.

Exposure assay: plants, insects and reptiles

Plants exposure

Lettuce seeds (*Lactuca sativa*) were obtained from Johnny's Selected Seeds (Winslow, ME). The seeds were pre-germinated in vermiculite for 10 d prior to transplanting to soil. Seven replicate pots per treatment, each containing two lettuce seedlings (total of 112 plants per experiment) were planted at 4 cm depth and were grown for 70 d in Cu (NP, bulk and ion) unweathered and weathered soils at ambient temperature, approximately 30% relative humidity, and on a 16-h photoperiod (light intensity 120 μM m^{-2} s^{-1} photosynthetic photon flux). The plants were amended with DI water and 10 mL of 10% Hoagland's solution (Phytotechnology Laboratories, Shawnee Mission, KS) on the first and fifth week after transplantation. After 70 d exposure, plant

tissues were harvested, measured, weighed (for wet mass and % moisture content determination) and were refrigerated at 4 °C. A portion of the harvested root and shoot tissue was digested or extracted and analyzed for pesticide and Cu and pesticide content by ICP-MS and GC–MS, respectively, as described below. The remaining plant tissues were used to feed crickets (*Acheta domestica*); also described below.

Insect exposure

Three-week-old crickets were acquired from Fluker Farms (Port Allen, LA) and separated into groups of 20 individuals per container (Food Service Warehouse); each container was considered as an individual replicate, and there were 16 replicates per treatment (unexposed control, NP, bulk and ion), similar to our previous work (De la Torre et al., 2015). A portion of exposed lettuce leaf was weighed and used a food source for the crickets during a 15 d exposure. Additionally, a small piece of orange cube and quencher was added as needed to provide additional nutrients (De la Torre et al., 2015). Crickets' feces were collected at 7 and 15 d; the feces were analyzed for Cu content as described below. At 15 d, the crickets were depurated for 5 d with small pieces of orange cube in order to avoid starvation. After depuration, the crickets were either supplied to lizards as a food source or were stored in a freezer (−4 °C) until digestion.

Reptile exposure

Three-week-old lizards (*Anolis carolinensis*) were acquired from Carolina Biological Supply Company (Burlington, NC) and housed individually in plastic containers covered with a mesh. Three lizards (a total of 24 lizards) were kept under light for 14 h per day using a UVB and heat lamp and in the dark during 10 h per day using a red lamp to achieve a constant temperature (75–80 F). Lizards were supplied with two live crickets (previously exposed to Cu treatments) per day and containers were misted with water at least once per day. After 15 d of treatment, the lizards were depurated and supplied with control crickets (not exposed to Cu) for five days. The lizards feces were collected and analyzed for Cu content as described below. After depuration, lizards were harvested in compliance with the AVMA Guidelines for the Euthanasia of Animals (2013 edition) (IACUC P24-15). Briefly, lizards were placed into 1 L Nalgene bottles and approximately 50 mL of halothane light mineral oil solution in soaked cotton balls were added as an anesthetic. Once the lizards were unresponsive, a metal syringe needle was used to pith the brain and lizard was dissected (Hoops, 2015); the internal organs, body cavity and head were separated and stored at 4 °C until digestion.

Matrix digestion

At harvest, plant and animal tissues were rinsed with tap water, followed by a rinse with dilute nitric acid (HNO_3) (0.01 M) to remove surface-adsorbed Cu particles. Plant, cricket, lizard tissues and feces were oven dried at 100 °C, weighed, and transferred to 50 mL DigiPREP polypropylene Class "A" graduated digestion vessels (SCP Science, Champlain, NY). Two and a half milliliter of 65% HNO_3 acid were added to each vessel for a 30 min pre-digestion. Samples were then digested for 45 min at 115 °C on a hot block (SCP Science, Champlain, NY). One milliliter of hydrogen peroxide (Fisher Scientific, Pittsburgh, PA) was added and the samples were heated for an additional 20 min. After digestion, DI water was added to achieve the desired volume (50 mL for plants; 25 mL for crickets and lizard) and the samples were analyzed by inductively coupled plasma-mass spectrometry (ICP-MS; Agilent 7500ce, Santa Clara, CA) for Cu (63 amu) content as previously reported (Pagano et al., 2016).

Physiological analysis

Total chlorophyll (a + b) and carotene were measured as previously described (Servin et al., 2017); details may be found in the Supporting Information (SI).

Quantitative reverse transcription PCR (RT qPCR) analysis

In order to assess plant response to the different forms of Cu exposure, RT qPCR analysis was performed on genes involved in Cu^{2+} transport (del Pozo et al., 2010; Grotz & Guerinot, 2006) from W and U lettuce samples; details may be found in the SI.

Pesticide quantification

Standards of cis-chlordane (CC), trans-chlordane (TC), and trans-nonachlor (TN) were obtained from the Environmental Protection Agency (EPA) National Pesticide Standard Repository (Fort Meade, MD) or from Supelco (Bellefonte, PA). Five replicates of root or shoot samples were rinsed with tap and DI water to remove particulates. To quantify chlordane content, lettuce tissues were extracted by QuEChERS method and quantified by gas chromatography with mass spectrometry (GC–MS) as previously described (De la Torre-Roche et al., 2013a,b). Additional details may be found in the SI.

Micro-XRF and micro-XANES data acquisition

Micro X-ray fluorescence (μ-XRF) and micro X-ray absorption near-edge(μ-XANES) structure were used to analyze 30 μm cross sections of roots exposed to U and W CuO NPs after 70 d of exposure. Additionally, μ-XRF analysis was performed in 5 d depurated crickets previously fed for 15 d with lettuce exposed to W CuO NPs. At harvest, lettuce roots and crickets were rinsed with DI water, embedded into Tissue Tek resin (Sakura Finetek USA, Torrance, CA) and flash-frozen by submerging samples in a container with isopentane (Fisher Scientific, Pittsburgh, PA) and liquid nitrogen. Samples were axially sectioned to 30 μm thickness using a Microtome plus cryostat (Triangle Biomedical Sciences, Durham, NC) and mounted onto Ultralene window film. Insect samples were axially sectioned at the cricket's midgut abdominal region. Samples were lyophilized for 48 h and stored at room temperature until analysis. Micro-XRF mapping of Cu K-edge was performed with a 9.2 keV incident beam at beamline ID21 of the European Synchrotron Radiation Facility (ESRF, Grenoble, France). The beam was focused with the use of KB mirrors to a size of $0.5 \times 0.9\ \mu m^2$ ($V \times H$). The fluorescence signal was detected using an 80-mm^2 active area SGX Si drift detector with a Be window. Two photodiodes were used to measure the incident and transmitted beam intensities. Maps were performed with a 100 ms dwell time and pixel size of 3–0.8 μm step size. The μ-XRF data were processed using the PyMCA software (Sole´ et al., 2007). For μ-XANES data acquisition, the energy was selected using a Si111 monochromator and scanned from 8960 to 9040 eV. The final Cu K-edge spectra were the sum of 3–5 individual scans with 0.1 s integration time and 0.5 eV resolution step. Reference materials CuO, Cu_2O and Cu_2S (Sigma, St. Louis, MO) were analyzed for controls as powder pellets in transmission and fluorescence mode.

Statistical analysis

A one-way ANOVA was performed followed by Tukey-HSD or Student–Newman–Keuls Multiple comparison test when comparing treatments. All tests were performed using the statistical package SigmaPlot 13. Statistical significance was based on

probabilities of $p \leq 0.05$. Network analysis was performed using the GeneMANIA data service (http://www.genemania.org/). The R software (https://www.r-project.org/) was used for the gene clustering of the U and W treatments.

Results

Trophic transfer to terrestrial food chains

Plant uptake of weathered and unweathered CuO NP, bulk and ion

The Cu content in roots and shoots from lettuce grown in soil amended with weathered (W) or unweathered (U) bulk or NP CuO and ions was determined. The data show the Cu shoot content was not significantly affected by exposure type or weathering (Figure 1(A)). Leaf tissues from the U treatments ranged from 6.0 (±1.9) (control-unexposed) to 6.8 (±1.5) (NP) mg/kg. Leaves from the W treatments ranged from 7.0 (±3.0) (control-unexposed) to 9.0 (±1.7, 1.6) (NP and ion, respectively) mg/kg. The accumulation of Cu in lettuce roots from in U or W soils is shown in Figure 1(B). Unlike the leaf tissue, the Cu content in lettuce roots from W and U exposures did vary with treatment, both by Cu type and by weathering (Figure 1(B)). Lettuce root Cu concentrations from the U treatments ranged from 60.2 (±25.2) (control-unexposed) to 152.2 (±69.9) (NP) mg/kg. Levels in the bulk and NP-exposed roots were significantly greater than controls (non-Cu exposed) and ion-exposed tissues, although not from each other. Roots from W treatments ranged from 13.5 (±6.0) (ion) to 326.6 (±59.1) (NP) mg/kg. Again, control (non-Cu exposed) and ion-exposed roots contained equivalent amounts of Cu; the bulk exposed roots had significantly less Cu and the NP-exposed tissues were significantly higher than the negative control. Interestingly, upon weathering the root content from bulk and ionic exposures significantly decreased by 35 and 81% (*t*-test; $p < 0.05$), respectively, but in the NP exposure, weathering resulted in a 53% increase in Cu accumulation. SI Figure S1 displays the total plant Cu content (μg) of lettuce plants, showing similar amounts of Cu among U treatments. However, as seen in SI Figure S1, weathering is generally decreasing Cu content in the control (unexposed), bulk and ionic exposures; conversely, weathering of the NP treatment is increasing Cu content of the plants. Similar to the concentration data, this suggests that a NP-specific transformation is occurring in soil and that this may significantly impact availability to the food crop.

Trophic transfer-primary consumers

After depuration for five days, the Cu accumulation in crickets that were fed for 15 d with lettuce exposed to U and W-Cu treatments was evaluated and is shown in SI Figure S2. The level of Cu present in the cricket tissues did not differ significantly with exposure type or weathering. Notably, the Cu content of control crickets (non-Cu exposed) was statistically equivalent to crickets consuming lettuce from the various Cu exposures. The Cu content of crickets from U treatments ranged from 16.6 (±3.6) (bulk) to 19.6 (±4.8, 3.1) (NP and ion, respectively) mg/kg. Upon exposure to the W treatments, the Cu cricket levels ranged from 18.8 (±5.6) (control-unexposed) to 22.1 (±5.3) (bulk) mg/kg.

Cu localization on cricket cross-sections from W-NP treatments was evaluated by synchrotron μ-XRF analysis. Figure 6(A) displays the tricolor μ-XRF image from cricket samples previously fed with lettuce grown in W-NP soils at 400 mg/kg; the red color indicates the presence of Cu within the cricket's abdominal region, the blue color displays P and the green color represents S. Figure 6(B–D) shows the temperature maps of the Cu, P and S, respectively, from cricket's abdominal region. As seen in the μ-XRF images, Cu was localized in the abdominal region of the cricket (Figure 6(A)) from W treatments. Interestingly, as seen in Figure 6(C,D), the distribution of P and S seems to be homogenous among cricket's digestive system (bottom structures on the figure) and abdominal region, whereas Cu is more localized and not associated with the cricket's digestive system (Figure 6(B)).

The Cu concentration in the feces did not differ between the two sampling periods and as such, data for the 7 and 15 d collections were pooled for statistical analysis across treatment and weathering time (Figure 2). The fecal Cu content from the U treatments ranged from 8.01 (±0.93) (unexposed control) to 13.66 (±7.81) (NP) mg/kg. The Cu accumulation in cricket's feces from the W treatments ranged from 10.26 (±0.64) (ion) to 14.1 (±2.37) (NP) mg/kg. In the U exposure, the Cu content in feces from the NP-exposed crickets was significantly higher than the other exposures. However, in the W exposure, fecal Cu content did not vary significantly with particle type. When directly comparing the effect of weathering, the fecal Cu content from the control (non-Cu exposed) and bulk treatments was significantly higher in the weathered exposure. Conversely, for the NP and ion treatments, weathering had no impact on Cu content. Last, we note that the cricket tissue and fecal Cu content were quite similar, ranging from 16.6 to 22.1 mg/kg and 7.93 to 14.1, respectively.

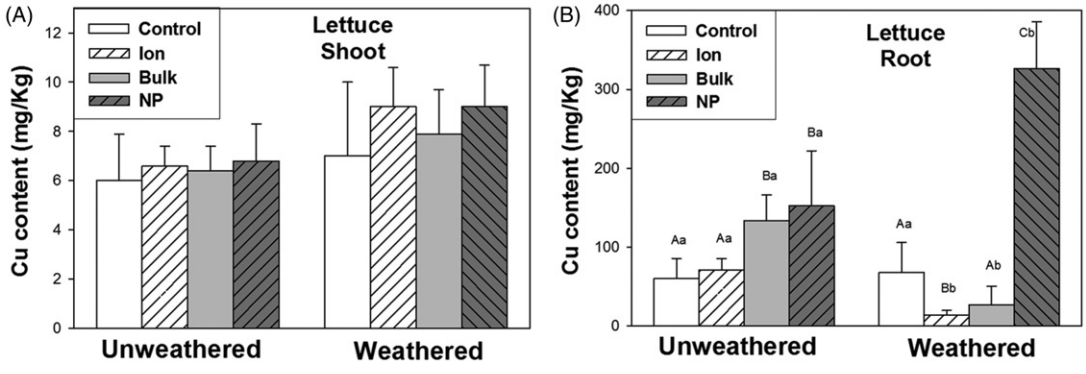

Figure 1. (A) Shoot and (B) root Cu content in lettuce plants (*L. sativa*) grown in soil amended with unweathered and weathered (70 d) 400 mg/kg Cu treatments. Different uppercase letters among columns indicate statistically significant differences within the same "age" group but across exposure/particle type (Control, NPs, Bulk and Ion) (one-way ANOVA with a SNK multiple comparison test). Different lowercase letters among columns indicate statistically significant differences between unweathered and weathered treatments of the same Cu type (*t*-test; $p < 0.05$). Absence of uppercase letter indicates no significant differences between treatments. Error bars represent standard deviation.

Cu content in secondary consumers

To evaluate the possible transfer of Cu to secondary consumers, lizards (*Anolis carolinensis*) were fed for 2 weeks with crickets that had consumed U or W control (non-Cu exposed)-, NP-, bulk- or ion-exposed lettuce. After depurating the lizard for five days, the Cu content in lizard intestine, body (muscle, bones) and head was determined (SI Figure S3A). Although the content did vary across the different tissue types (intestine consistently higher than the body or head), the amount of Cu in a given tissue did not vary significantly with exposure type or weathering. The Cu content in lizard intestinal tissues from U exposure ranged from 9.9 (bulk) to 17.9 (ion) mg/kg; the W treatments ranged from 9.1 (NPs) to 22.2 (ion) mg/kg. The Cu content in the lizard body from U and W exposures ranged from 2.2 (NPs) to 2.5 (bulk and ion) and 1.7 (bulk) to 5.9 (NPs) mg/kg, respectively. Also, the head Cu content ranged from 1.8 (ion) to 2.1 (unexposed control) mg/kg in the U exposure and from 1.4 (unexposed control) to 2.0 (ion) mg/kg in the W exposure.

Lizard's feces were collected during the exposure period and the Cu content was evaluated (SI Figure S3B). Similar to the lizard tissues, fecal Cu content did not vary significantly with exposure type or weathering. For the U exposure, the Cu content in feces ranged from 43.7 (±7.2) (ion) to 52.1 (±22.3) (bulk) mg/kg. For the W exposure, Cu content ranged from 40.9 (±2.5) (ion) to 952.4 (±479.6) (bulk) mg/kg. The relatively consistent levels found across all treatments in the unweathered treatment is particularly notable when compared to the weathered exposure, where variability among replicate samples from the bulk and NP treatments was dramatically greater. Due to the variability, these differences are not statistically significant but they may be worthy of further investigation.

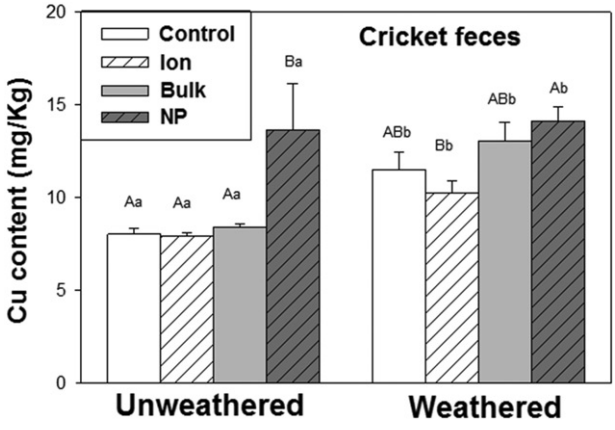

Figure 2. Fecal Cu content from crickets consuming lettuce exposed to unweathered or weathered bulk or NP CuO at 400 mg/kg or ionic Cu at 40 mg/kg. Feces collected after 7 and 15 d did not differ significantly and were pooled by treatment. Bars with different uppercase letters are significantly different within an exposure (unweathered or weathered) and across Cu types (Control, NPs, Bulk and Ion) (one-way ANOVA on ranks followed by a SNK multiple comparison test). Bars with different lowercase letters are significantly different with a Cu type but across exposure (unweathered versus weathered) (Mann–Whitney rank sum test). Error bars represent the standard error of pooled data.

Effects of Cu unweathered and weathered treatments on L. sativa

Micro-XRF and micro-XANES data analyses

The spatial distribution and speciation of Cu on lettuce root cross-sections from U-NP and W-NP treatments were evaluated by synchrotron μ-XRF and μ-XANES analysis. Figures 3(A) and 4(A) display the tricolor μ-XRF images from root exposed to U- and W-NP soils at 400 mg/kg, respectively; the red color indicates the presence of Cu on the vascular region, the blue color displays K and the green color represents Ca. Figures 3(B) and 4(B) show the temperature maps of the Cu-K fluorescence line. Figures 3(F–H) and 4(C,D) show the fluorescence images from the main root (MR) and secondary

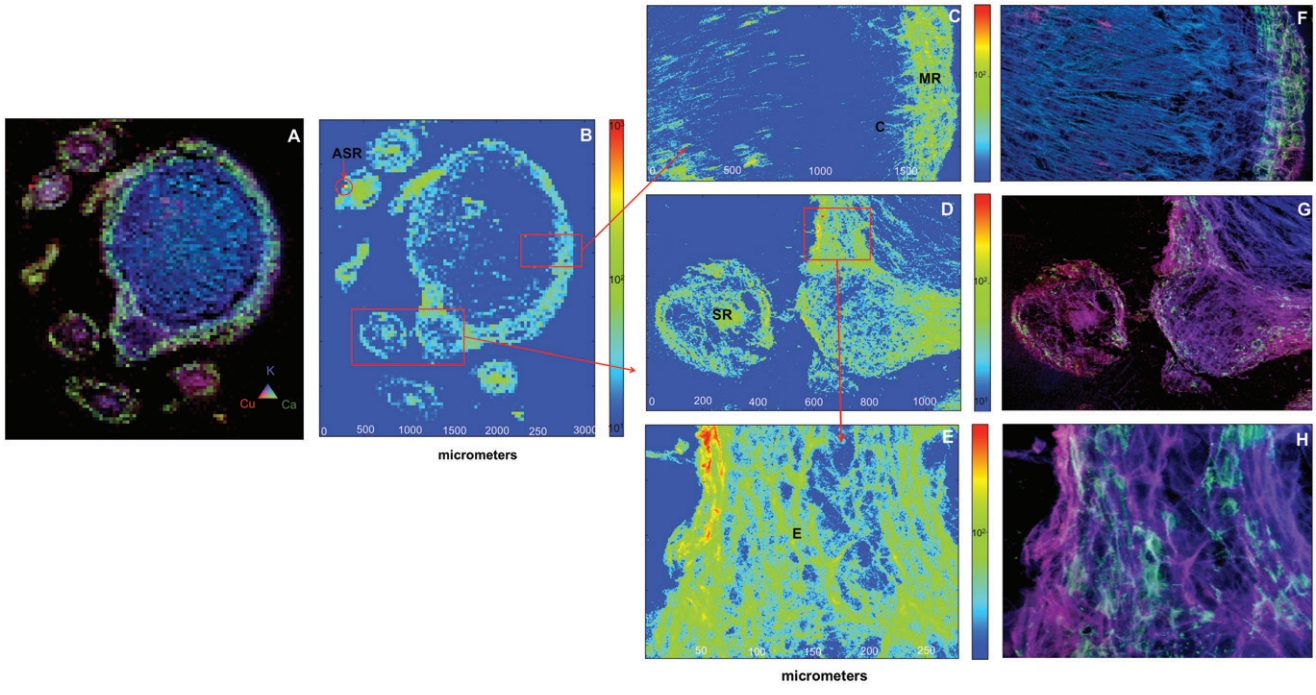

Figure 3. Images of lettuce root cross section exposed to weathered CuO NPs at 400 mg/kg for 70 d. (A) Tricolor micro-XRF maps of root cross sections, red color stands for Cu, blue for K, and green for Ca. The μ-XRF map was acquired at 9.2 keV, 100 ms dwell time, 3–0.8 μm^2 pixel size. (B) Cu temperature map, color scale units are raw intensity; areas where μ-XANES was acquired from ASR: aggregate sec. root; SR: secondary root; E: epidermis; MR: main root and C: cortex are indicated. (C–E) Cu temperature map of main and secondary roots, color scale units are raw intensity. (F–H) μ-XRF maps from main and secondary roots.

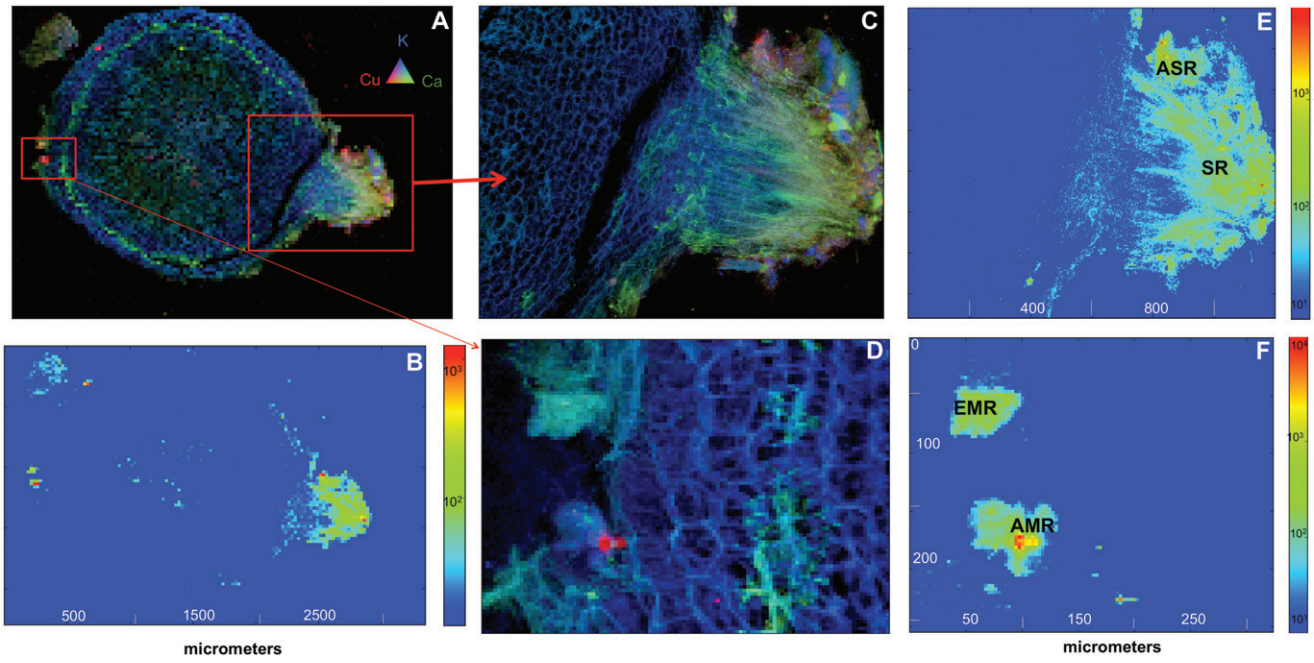

Figure 4. Images of lettuce root cross section exposed to unweathered CuO NPs at 400 mg/kg for 70 d. (A) Tricolor micro-XRF maps of root cross sections, red color stands for Cu, blue for K, and green for Ca. The μ-XRF map was acquired at 9.2 keV, 100 ms dwell time, 3–0.8 μm^2 pixel size. (B) Cu temperature map, color scale units are raw intensity. (C, D) μ-XRF maps from main and secondary roots (E, F) Cu temperature map of main and secondary roots from (C, D) μ-XRF maps, color scale units are raw intensity. Areas where μ-XANES was acquired from ASR: aggregate sec. root; SR: secondary root; EMR: epidermis main root and AMR: aggregate main root are indicated.

roots (SRs), respectively. Additionally, Figures 3(C–E) and 4(E,F) show the temperature maps of main and SRs from Figures 3(F–H) and 4(C,D), respectively. As evident in the μ-XRF images, Cu was localized in the main and SRs (Figures 3(A) and 4(A)) of the exposed lettuce plants, regardless weathering conditions. Interestingly, as seen in Figure 3(A) the distribution of Ca (green color) was altered due to weathering conditions, showing a more even distribution within the MR from the W exposure (Figure 3(A)) as compared to the U treatment (Figure 4(A)). Additionally, a more localized Cu distribution was observed in the U treatments (Figure 4(B)); in the W exposure, the Cu was more homogenously distributed within root tissue (Figure 3(B)).

In order to obtain information about the oxidation state of Cu present in lettuce roots, μ-XANES of the Cu K edge was used. Figure 5 displays the weight of components from XANES linear combination analysis and μ-XANES spectra of reference materials and selected spots obtained from epidermis, SRs, MR, cortex and aggregates of SRs where Cu was localized (Figures 3 and 4). As seen in Figure 5, μ-XANES spectra obtained from the different root areas of the W treatment were completely reduced (no CuO detected) and present as Cu_2O and/or Cu_2S. For example, aggregates from the SRs from weathered treatments were mostly present as Cu_2O (94.2%), with some minor reduction to Cu_2S (5.7%) (Figure 5). Conversely, W Cu localized in epidermis (E) was still completely reduced but present more equally as Cu_2O (45.9%) and Cu_2S (43.5%); a similar distribution was present in root cortex area (C), with Cu_2O at 46.4% and Cu_2S at 48.3%. Interestingly, Cu localized in the SR and MR was mostly found as Cu_2S, 62.3% and 85.1%, respectively, with Cu_2O present in a lower percentage (34.0% and 8.7%, respectively). However, roots from U-NP treatments showed a different scenario, with the original oxidized Cu being detected in multiple tissues. For example, Cu aggregates in secondary (ASR) and main root (AMR) closely resemble the spectra from the CuO reference material, suggesting that little transformation of the original CuO NP had occurred in these tissues during the exposure period. Conversely, Cu localized in epidermis (EMR) area was found as CuO (31.4%), Cu_2O (23.8%) and Cu_2S (44.7%). Similarly, Cu localized in SR was present as both oxidized and reduced forms. These findings suggest that significant transformation of CuO NP occurred in the soil during the weathering period and that this altered elemental speciation significantly impacted Cu accumulation by the plant (Figure 1).

Physiological effects of Cu unweathered and weathered treatments

Cu exposure had limited impacts on lettuce biomass. For both the U exposures, total plant biomass was not significantly different as a function of bulk or NP CuO or ion exposure. Total plant mass ranged from 9.1 g (wet mass, U ion) to 11.4 g (U unexposed control). However, the root biomass of NP-exposed plants was significantly less than that of the bulk treatment; no other tissue-specific differences were evident. In the W exposure, the total biomass ranged from 8.2 g (W NP) to 9.5 g (unexposed control); in addition, the NP- and ion-treated plant biomass was significantly less than the unexposed controls. With regard to individual tissues in the W exposure, there were no differences of significance in the root biomass but similar to total mass, the shoot weight of NP- and ion-treated plants were significantly less than the unexposed control plants.

SI Table S1 shows the length of lettuce root and shoot tissues upon exposure to U and W Cu (bulk, NP) at 400 mg/kg or ionic Cu at 40 mg/kg soil. The root and shoot moisture content and leaf photosynthetic pigment contents of the plants are shown in SI Tables S2 and S3, respectively. As seen in Table S1, the U treatments did not cause overt toxicity in exposed lettuce shoots; however, root length in the CuO NP and bulk exposure was significantly decreased relative to unexposed controls. Interestingly, the ratio of root to shoot length seemed to change with weathering. For the weathered condition, the shoots tended to be larger and the roots tended to be smaller. For example, the

Unweathered					Weathered				
	Components					Components			
Root region	CuO	Cu_2O	Cu_2S	R-factor	Root region	CuO	Cu_2O	Cu_2S	R-factor
ASR	1	0.000	0.000	0.000	ASR	0.000	0.943	0.058	0.0009
EMR	0.314	0.238	0.447	0.009	E	0.000	0.460	0.435	0.0009
SR	0.658	0.342	0.000	0.004	SR	0.000	0.340	0.624	0.0029
SR	0.00	0.554	0.446	0.002	MR	0.000	0.088	0.851	0.0019
SR	0.458	0.355	0.187	0.001	C	0.000	0.465	0.484	0.0029
SR	0.635	0.43	0.000	0.006					
SR	0.229	0.353	0.417	0.004					
AMR	1	0.000	0.000	0.000					

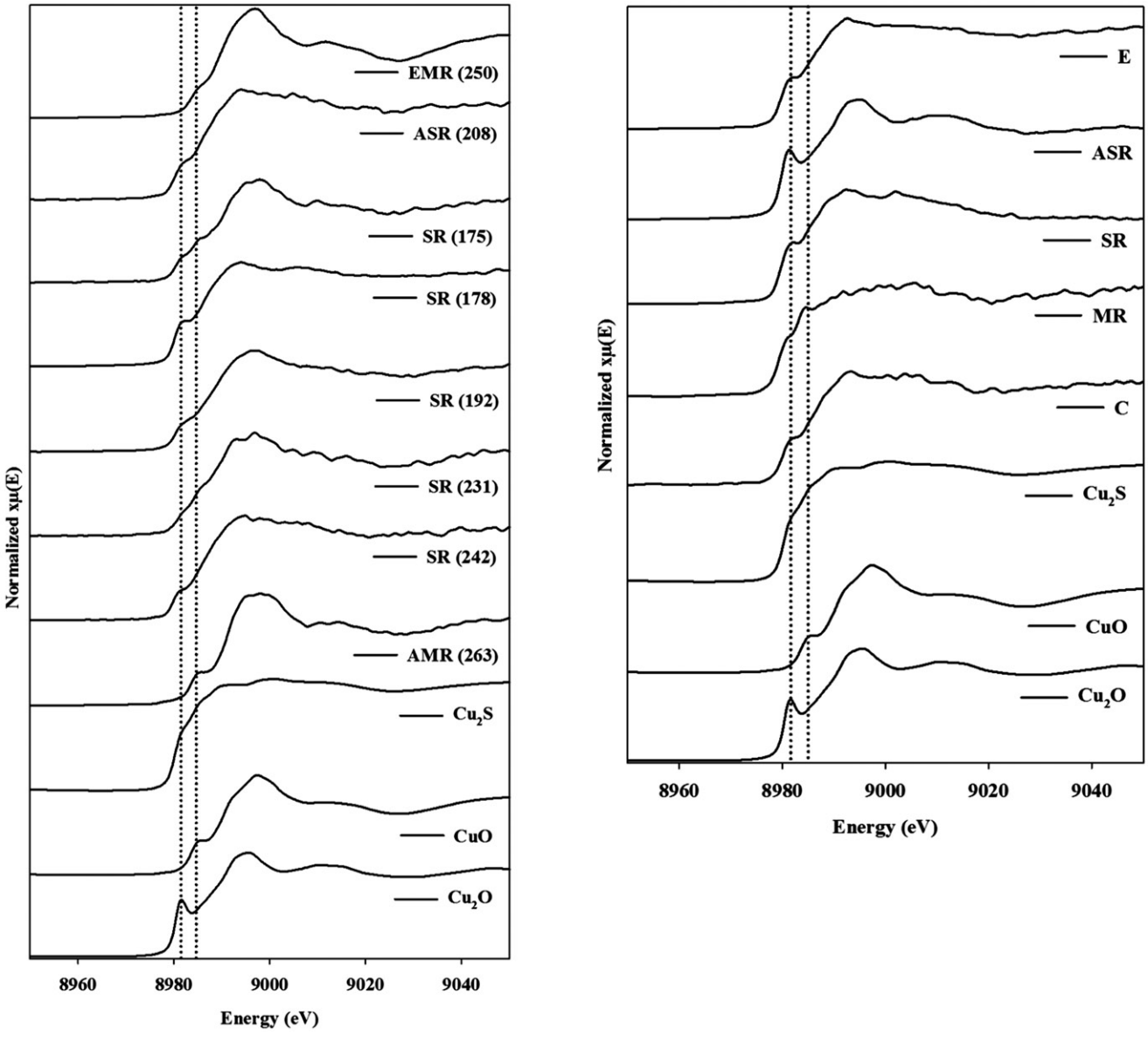

Figure 5. Weight of components from XANES Linear combination analysis tested in ASR: aggregate sec. root; SR: secondary root; EMR: epidermis main root; AMR: aggregate main root; E: epidermis; MR: main root; C: cortex. μ-XANES spectra of CuO, Cu_2S and Cu_2O reference materials and spots of interest (from Figures 3 and 4) of roots exposed to unweathered and weathered CuO NPs at 400 mg/kg for 70 d.

ratio of root to shoot length ranged from 0.42 to 0.70 for the U treatment and from 0.28 to 0.37 for the W treatment. In the W exposure, the reverse trend was noted; Cu exposure had no impact on root length but for the shoots, both the NP and bulk exposure exerted significant toxicity. The moisture content of the lettuce tissues was largely unaffected by treatments, with the exception of the W bulk exposure where moisture decreased significantly compared to respective unexposed controls (SI Table S2). The chlorophyll *a*, chlorophyll *b* and carotene content were not affected by Cu exposure or weathering (SI Table S3).

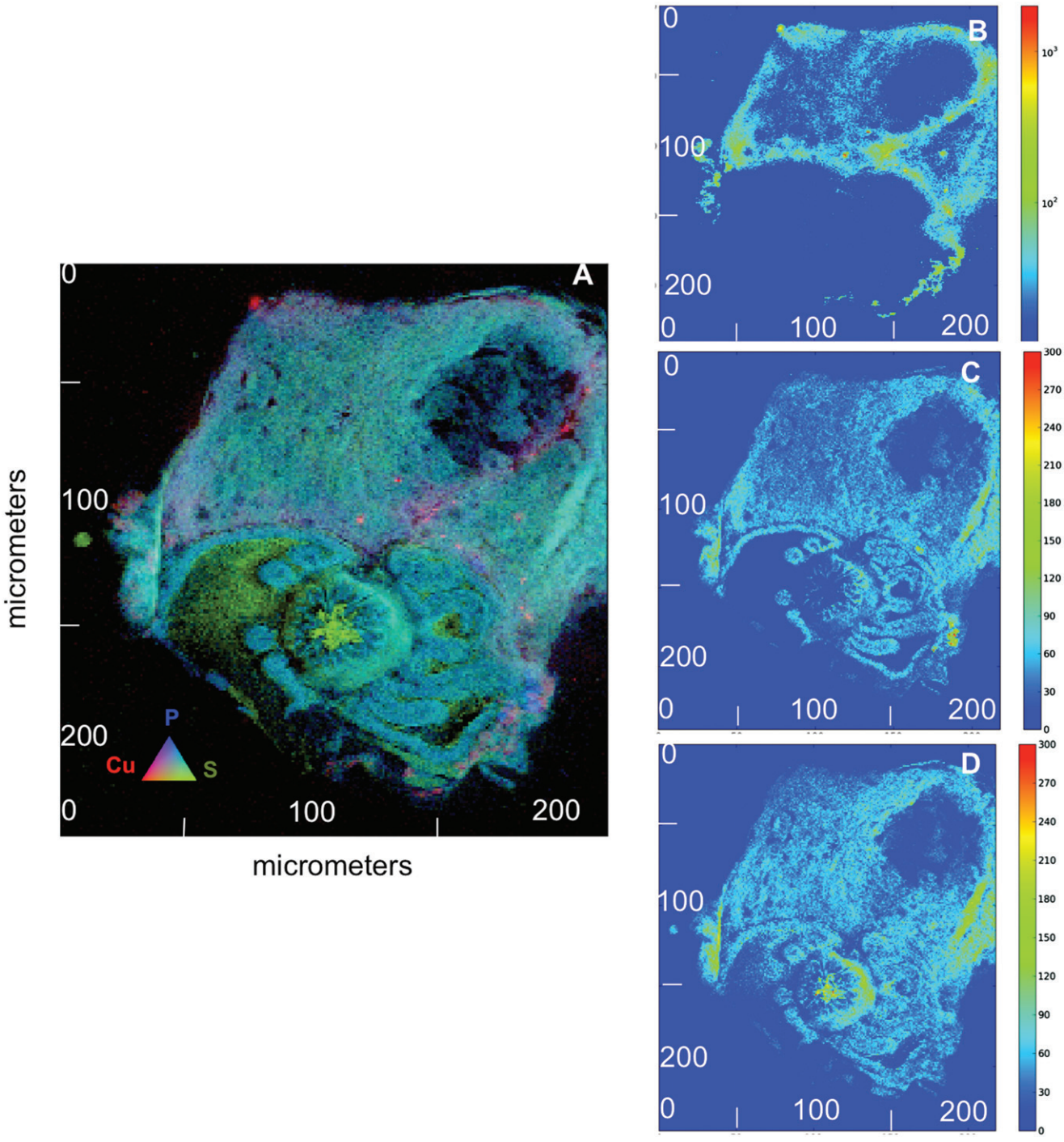

Figure 6. Images of cricket cross sections exposed to lettuce grown with weathered CuO NPs at 400 mg/kg for 70 d. (A) Tricolor μ-XRF maps of cricket cross sections; red color is Cu, blue is P, and green is S. The μ-XRF map was acquired at 9.2 keV, 100 ms dwell time, 3–0.8 μm^2 pixel size. (B) Cu temperature map, (C) P temperature map, and (D) S temperature map of cricket cross section; color scale units are raw intensity.

L. sativa molecular response to Cu exposure

Expression analysis was performed on nine *L. sativa* ortholog genes of *A. thaliana* that are known as to be involved in Cu^{2+} uptake (SI Table S4 and SI Figure S4); notably, the form of Cu significantly impacted the expression profile (SI Figure S5). For the Cu ion exposure, a general up-regulation of most of the genes analyzed (compared to the unexposed controls) was observed, although the intensity of the up-regulation was greater in the U treatment. The lone exception to this trend of upregulation is *LsHMA1* (heavy metal ATPase), whose expression level was not significantly different from the unexposed control; this suggests that Cu^{2+} concentration was not high enough to trigger the *LsHMA1* modulation (Boutigny et al., 2014). In the W ion treatment, the down-regulation of the *LsCCH* gene (copper chaperone) was reported for *LsATX1* (whose gene product is involved in Cu^{2+} transport), expression was not different from the control (non-Cu exposed); both genes are involved in the intracellular Cu delivery system (Himelblau & Amasino, 2000). Importantly, in the bulk and NP exposures, the expression profile was significantly different from that of the ion. Under CuO bulk and CuO NPs treatments, a general trend of down-regulation of all the genes was evident compared to the unexposed controls. Unlike the ion, weathering

did not lessen the magnitude of these effects; no significant differences were observed between bulk and NPs treatments in W and U treatments. These results confirmed the unique molecular mechanisms involved in the Cu^{2+} response relative to bulk or NP exposure.

Pesticide content in L. sativa

The impact of NP, bulk, and ionic Cu on the uptake and translocation of weathered chlordane by lettuce was determined. The concentration of weathered TC, CC, and TN in the soil was 752 μg/kg (±27.9), 927 (±37.4) μg/kg, and 445 μg/kg (±20.5), respectively (see SI for more information). No pesticide residues were detected in the shoots. In the U exposure, the root content of total chlordane (sum of CC, TC, TN) did not vary as a function of Cu type and ranged from 6260 μg/kg (ion) to 13,540 μg/kg (bulk). In the weathered exposure, the general trend was that Cu-treatment decreased chlordane uptake, although the effect was only statistically significant in the bulk ($p = 0.056$) and ion treatments ($p = 0.05$). The concentration of total chlordane for the control (non-Cu exposed), NP, bulk, and ion exposures were 22,600 (±9320), 16,420 (±5270), 10,020 (±8760), and 11,000 (±3128) μg/kg, respectively. When directly comparing the impact of weathering across a Cu-treatment type, CuO NP co-exposure significantly increased chlordane uptake as a function of residence time in soil; no other significant differences were noted. For additional comparison, the absolute amount of each chlordane component in the root tissues was calculated (SI Figure S6).

With regard to the absolute amounts (total ng) of the individual chlordane components, there were no differences of statistical significance as a function of Cu type or weathering. The roots from the U exposure contained the greatest amount of CC, ranging from 1010 ng (ion) to 2240 ng (bulk), while in W-treatments ranged from 1608 ng (ion) to 3397 ng (control) (Figure S6). Trans-chlordane levels ranged from 625 (NP) to 1211 ng (bulk), and from 879 ng (ion) to 1899 ng (control) in U and W treatments, respectively. Trans-nonachlor content in U exposure ranged from 299 (NP) to 678 ng (control); the W exposure had a TN content ranging from 479 ng (ion) to 1261 ng (control). The levels of each chlordane component in the root tissues correlated well with the detected amounts in soil, indicating that residues did not selectively translocate. Similar nonselective translocation results were found previously in zucchini, tomato, corn, and soybean plants (De la Torre-Roche et al., 2013a,b).

Discussion

Aging effects on the Cu accumulation in L. sativa

In the present study, we reported a higher Cu content from U-NP and W-NP experiments in lettuce roots when compared to control (non-Cu exposed) and other Cu (bulk and ion) treatments (Figure 1(B)). Other studies have reported a higher accumulation of Cu when exposed to NPs treatments in comparison to corresponding bulk and ionic materials. For example, Wang et al. (2012) reported higher Cu content in maize (*Zea mays* L.) roots and shoots upon hydroponic exposure to CuO NPs (20–40 nm) at 100 mg/L when compared to Cu^{2+} and CuO bulk treatments. Similarly, Trujillo-Reyes et al. (2014) reported a higher accumulation of Cu in lettuce roots when exposed to Cu/CuO NPs suspensions for 15 d at 10 and 20 mg/L in comparison with ion treatments. These studies suggest that nanoscale size results in greater Cu accumulation in plants, either through direct NP uptake or from greater ion release as a function of size (or both). However, our results demonstrated that Cu translocation to lettuce shoots was not significantly affected by particle type, suggesting that Cu translocation may be tightly regulated in this species. Hong et al. (2015) reported that lettuce translocated only 0.5–0.6% of Cu from roots to shoots upon exposure to 0–20 mg/L Cu NPs/compounds, whereas 3–5% was translocated in alfalfa, suggesting that Cu uptake and translocation is plant specific. In our study, shoot Cu levels were from 2 to 10% of the root concentration in all exposures except the W ion treatment, where leaf concentrations were 66% that of the root value. All of these findings are in general agreement with previous studies that have reported a lower Cu accumulation in edible shoot tissues in comparison with roots, which is due to limited mobility of Cu within the vascular tissues (Ginocchio et al., 2002).

Interestingly, Cu accumulation in plant roots was significantly affected by weathering conditions, with the particle types responding differently. For example, weathering significantly decreased Cu root content in the bulk particle treatment, but the reverse was true for NP CuO, where weathering more than doubled Cu root concentrations (Figure 1(B)). In terrestrial systems, plant roots excrete organic acids and other exudates to facilitate nutrient acquisition from soil (Lopez-Bucio et al., 2000). These organic acids will alter the rhizosphere abiotic and biotic conditions in ways that may significantly enhance or inhibit element dissolution, thereby altering the availability and mobilization of NPs. Mudunkotuwa et al. (2012) investigated the effect of aging and organic acid/ligand presence on the fate of Cu-based NPs. The authors reported that the ligand-promoted dissolution of CuO NPs was inversely related to pH and resulted in greater Cu mobility due to the formation of ions and smaller NPs in the presence of the organic acids. Our molecular results did confirm changes in the expression level of genes involved in Cu transport and detoxification for the ion exposure; however, no such changes were noted for the NPs and bulk treatments, where dissolution may have still been too low to trigger a response. Importantly, our μ-XANES analysis clearly indicates that weathered CuO NPs are reduced from Cu (II) to Cu (I), undergoing sulfidation after time dependent ion dissolution in the soil. This likely explains the higher Cu content in roots from the weathered exposure relative to the U NPs treatment where significantly greater untransformed CuO was found (Figure 5). The adsorption of organic acids and other biomolecules from plants or other biota in soil may drive NP dissolution/transformation processes and that subsequently increase particle mobility and bioavailability to plants.

Trophic transfer of Cu unweathered and weathered

In the present study, the transfer of Cu from lettuce shoots to primary and secondary consumers was measured but was found to not vary significantly with weathering or particle type. In fact, Cu levels observed in the cricket and lizard tissues were statistically equivalent to the unexposed controls (SI Figure S2 and SI Figure S3). The Cu content in cricket tissues from the U exposure was 2.6–3 times higher than leaf tissues that were consumed, while cricket Cu concentration in the W exposure was 2.2–2.8 times greater than the consumed lettuce; these values are not significantly different. The fact that the control (non-Cu exposed) and Cu-treatment samples did not differ significantly in the crickets is not surprising given that the levels in the lettuce shoots did not vary by Cu type. Holbrook et al. (2008) reported similar results with quantum dot (QDs) trophic transfer studies involving bacteria and ciliates; limited bioaccumulation and no biomagnification were observed. Interestingly, the Cu content of the cricket's feces showed different patterns between the U and W exposures. In the

U exposure, the fecal content in the NPs treatment contained significantly more Cu than the unexposed control, bulk and ion treatments. Given that the tissue amounts were equivalent, this suggests a potentially higher initial Cu accumulation in NP-exposed crickets but that this greater burden was later eliminated during the five-day depuration period (SI Figure S2).

This highlights a particle size-dependent difference in the transfer, accumulation and elimination of Cu; this is quite unexpected given the equivalent levels of Cu in all consumed lettuce tissues, regardless of Cu treatment type. Notably, the Cu content in the insect tissues ranged from approximately 17 to 22 mg/kg and the fecal Cu content was less, ranging from 8 to 15 mg/kg. This pattern of less element content in the feces differs from some of our previous trophic transfer work. In a study evaluating bulk and NP La_2O_3 trophic transfer from soil to lettuce and crickets, we reported lower La content in the insect tissues after 7 d depuration as compared to 48 h depuration; however, levels in the feces were still at least 10-times greater than that of the tissues (De la Torre et al., 2015). Similarly, in a set of experiments involving bulk and NP CeO_2 transfer from soil to zucchini (*Cucurbita pepo*) to crickets; Ce content in the feces was 10–20 times greater than that retained within the organism (Hawthorne et al., 2014). The reasons for this element-specific difference in elimination are not known but are mostly likely related to the fact that Cu is a required nutrient, whereas Ce and La have no known biological function. However, in a more recent study involving kidney bean (*Phaseolus vulgaris* var. red hawk) and Mexican bean beetles (*Epilachna varivestis*) exposed to bulk and NP CeO_2, the ratio of Ce content in the tissues to feces depended greatly on life stage of the beetle. In the larval form (7 d), the fecal Ce content was nearly 30 times higher than the tissues but when measured at the adult stage (21 d), tissue content was actually greater than that found in the feces (Majumdar et al., 2016). Our μ-XRF analysis showed a clear accumulation of Cu within the cricket's abdominal region in insects from W-CuO treatments. As seen from these images, Cu is not present in the insect's intestines; P and S presence is clearly observed within the digestive system (6C and D). This confirms the elimination of Cu from the cricket's gut during the 5 d depuration process. However, due to the lack of beamtime to test further conditions, it is not possible to differentiate this distribution from non-CuO NP exposed crickets or to conclude the speciation of Cu within cricket's tissues. This does however raise some interesting questions over NP distribution within the insect that are currently topics of ongoing investigation.

As noted above, the secondary consumer (*Anolis carolinensis*) data was similar to the crickets they consumed; Cu content did not differ significantly with weathering or Cu treatment. Copper was detected in all organs tested but levels were statistically equivalent to the unexposed controls (SI Figure S3 A). The highest concentration of Cu was detected in the lizard's intestine, with the body (muscle/bone) and head accumulating less but comparable amounts. In addition, the Cu content in lizard feces did not differ with weathering or Cu treatment (SI Figure S3 B). As was mentioned previously, the exposed crickets were depurated for a 5 d period before presentation to the lizards and at that point, all herbivores, including unexposed controls, had statistically equivalent levels of Cu. As such, particle size-dependent transfer of either Cu to the lizards or of elimination by the lizards was not anticipated. These findings agree in part with select studies focusing on the trophic transfer of engineered NPs in terrestrial systems, although the current literature is somewhat mixed on this topic. For example, De la Torre et al. (2015) showed that the transfer of bulk and NP La_2O_3 from soil to lettuce to crickets to mantids did not differ with particle size, although the levels of both treatments were significantly above the unexposed controls. Conversely, Judy et al. (2011) demonstrated the transfer and biomagnification of Au NPs from tobacco leaves (*Nicotiana tabacum* L. cv *Xanthi*) to tobacco hornworms (*Manduca sexta*). Similarly, Majumdar et al. (2016) demonstrated transfer and biomagnification of NP CeO_2 from exposed kidney bean (*Phaseolus vulgaris*) leaves to adult bean beetles (*Epilachna varivestis*); notably, biomagnification was not evident in the younger larval and pupal life stages. Interestingly, Unrine et al. (2012) conducted a follow up study with Au NPs in a different model food chain, and noted that although the NPs were transferred from earthworms (*Eisenia fetida*) to bull frogs (*Rana catesbeina*), a significant decrease concentration was observed in the consumer. These findings agree with a previous study from our group where although the transfer of Ce from soil to zucchini to crickets and spiders did differ as a function of CeO_2 particle size (NP yielded greater Ce content), the concentration declined by an order of magnitude or more at each subsequent trophic level (Hawthorne et al., 2014). These results highlight the contradictory yet limited literature in this area. However, they do demonstrate that NP accumulation, transfer, and biomagnification can occur within terrestrial food chains but this depends greatly on particle type, species, and exposure conditions.

Biological impacts of unweathered and weathered Cu in L. sativa

In this study, synchrotron analysis was performed to compare and evaluate the speciation of Cu in lettuce roots from W and U-NPs treatments. In both exposures, μ-XRF analysis confirmed the presence of Cu in the secondary and primary roots of lettuce plants. However, weathering condition did impact the distribution of both Cu and Ca within root tissues. Roots from the U-NP treatments showed a more localized distribution of Cu within the roots (Figure 4(A)) when compared to the weathered exposure, where Cu has a markedly more noticeable homogenous distribution (Figure 3(A)). In the present study, the overall uptake of plant nutrients was not evaluated by ICP-MS; however, the μ-XRF images (Figure 3(A)) from lettuce roots treated with W-NP also showed a more homogenous distribution of Ca within the root tissues when compared to the unweathered exposure. These findings suggest that weathering or aging time of NPs in soil could influence both particle and nutrient uptake and/or distribution in plants. This is in agreement with our Cu concentration data, where a higher Cu root content was observed in the W-NPs treatments as compared to the U-NPs (Figure 1). With regard to Ca, the element is an essential plant nutrient and has a role in cell wall and membrane structure; excess of Ca may cause toxicity and reduce growth rates (White & Broadley, 2003). Others have reported that NPs exposure can influence *in planta* nutrient distribution. For example, Larue et al. (2016) reported that exposure to 1000 mg L^{-1} of TiO_2 and Ag-NPs disrupted lettuce root homeostasis as a consequence of greater accumulation of Fe, P, S and Ca in the root epidermis. Zhao et al. (2015) used μ-XRF elemental maps of maize kernels to demonstrate that exposure to CeO_2 NPs caused differences in the distribution of Ca and other nutrients elements. Similarly, Trujillo-Reyes et al. (2014) reported significant increases in Zn, S and Ca concentrations in lettuce roots treated with Cu/CuO NPs and $CuSO_4$, suggesting that exposure significantly altered nutrient absorption and transport in plants. Notably, previous studies have indicated that Cu at high concentrations can damage plant membranes, thus enabling the entry of elements into the cell with little selectivity (Fernandes & Henriques, 1991). Although our understanding of NP-plant interactions is still

developing, our results clearly suggest that NPs aging/weathering conditions could impact the bioavailability and distribution of essential nutrients, and thus affecting nutritional quality of plants in natural environments. This is clearly an area in need of intense additional investigation.

The μ-XANES analysis from roots treated with W-NPs demonstrated significant Cu (II) reduction to Cu_2O and Cu_2S compounds in all selected areas (main and SRs, epidermis and cortex). By comparison, roots from the U-NPs roots contained Cu mostly as the original oxidized CuO, depending somewhat on root region (Figure 5). For example, the LC analysis of the μ-XANES spectra from W-NPs exposed aggregates from secondary (ASR) roots showed that 94.2% was present as Cu_2O, 5.7% as Cu_2S. Similar root areas from the U-NPs treatment showed that CuO remained in the original chemical form, with negligible biotransformation. Metal sulfidation has been proposed as a detoxification process for metallic NPs (Levard et al., 2011; Liu et al., 2010; Wang et al., 2013). Moreover, Wang et al. (2013) showed that CuO NPs undergo sulfidation through a sequential dissolution and re-precipitation mechanism that yielded secondary aggregates of CuS NPs (10 nm) that were active catalysts for bisulfide oxidation. Interestingly, the authors stated that under the time scale of their experiment, the formation of Cu_2S was not observed, suggesting slow phase transition of crystalline Cu_2S (Wang et al., 2013). Although CuO NPs are often referred to as insoluble materials, studies have demonstrated that CuO NPs release measurable amounts of soluble copper in relevant media (Wang et al., 2013). In another study, Wang et al. (2012) reported the transfer of CuO NPs from exposed shoots to root tissues, noting significant reduction to Cu_2S and Cu_2O during or after transport. Similarly, Dimkpa et al. (2012) reported the reduction of CuO to Cu (I)–sulfur complexes in wheat plants grown in sand. In the previously mentioned study, authors reported the majority of Cu (64%) was in the original form as CuO, while the remainder (36%) was bound to sulfur as a reduced Cu (I)–S species that formed as a result of normal plant physiological processes (Dimkpa et al., 2012). The reduction of Cu (II) to Cu (I) can be attributed to the reducing sugars in plants such as glucose and fructose, which are continually transported from photosynthetic cells to root tissue (Wang et al., 2012). This may partly explain the reduction to Cu (I) from our unweathered exposure, where some Cu (I) sulfur complex formation was observed in the epidermis and SRs tissues (Figures 4 and 5). However, in the weathered exposure, where Cu_2O and Cu_2S were predominantly present, the CuO reduction to Cu (I) complexes likely occurred in the soil during weathering/aging processes. Importantly, this suggests the biotransformation processes in the soil may result in increased availability of chemically altered NPs. The significance of this process to overall NP exposure and risk, as well as the mechanisms underlying the processes, remain topics of active investigation.

The production of chlorophyll *a*, *b* and carotenoids was not significantly impacted by weathering or Cu exposure. The literature on NP-interactions with the plant photosynthetic apparatus is mixed. In *A. thaliana* grown in agar medium, the total chlorophyll content was not affected by exposure to CuO NP at 0.5 and 1.0 mg/L; however, at higher concentrations (2.0–100 mg/l), pigment production was impacted in a dose dependent manner (Nair & Chung, 2014). In another study using a chlorophyll *a* fluorescence imaging technique, Perreault et al. (2010) showed that CuO NPs inhibit the photosynthetic process in *Lemna gibba* at 100–400 mg/L in microplate conditions; specifically, photosystem II quantum yields and photochemical quenching of fluorescence associated with electron transport were negatively affected, thereby decreasing plant growth. Conversely, Cu NP exposure at 0.05–1.0 mg/L for 15 d in an agar-perlite medium significantly increased chlorophyll and carotene contents in the leaves (Pradhan et al., 2015). More recently, Da Costa & Sharma (2016) exposed rice hydroponically to CuO NP for 24 days, and reported reduced levels of the photosynthetic pigments carotene, lutein and violaxanthin, as well as reduced numbers of thylakoids per granum. Clearly the literature on phytotoxicity as determined by pigment production is mixed; this is likely due to species and even life cycle specific responses, as well as differences in exposure and experimental design.

Phytotoxicity as measured by plant biomass or root/shoot length was somewhat limited and inconsistent. Root length reduction in lettuce was noted in the unweathered bulk and NP CuO treatment, although there were no impacts on biomass. Conversely, in the weathered exposure, total plant mass in the NP and ion exposures were reduced but there were no corresponding effects on length. Our findings are in general agreement with the literature. For example, Nair et al. (2014) reported that mung bean (*Vigna radiata* L.) root biomass and length were significantly reduced upon exposure of different concentrations (0–500 mg/L) of CuO NPs; however, shoot biomass and length were only reduced upon exposure to 200 and 500 mg/L of CuO NPs. Le Van et al. (2016b) reported that plant biomass of cotton was not affected at low (10 mg/L) concentrations of CuO NPs; however, shoot biomass was reduced at CuO NP exposure levels (1000 mg/L). Also, decreases of 75% of that of control in cucumber (*Cucumis sativus*) seedling biomass was reported upon exposure to 1000 mg/L of CuO NPs (Kim et al., 2012). Reductions in root and shoot growth have been reported in response to CuO NPs exposure in maize (Wang et al., 2012), wheat (Dimkpa et al., 2012), barley (Shaw et al., 2014) and rice seedlings (Shaw & Hossain, 2013). Nair & Chung (2014, 2015) also reported a reduced root growth in *Arabidopsis thaliana* and *Pisum sativum* (green peas) grown in agar medium containing 0.5 mg/L and 100 mg/L CuO NP exposure for 14 and 21 d, respectively. However, the authors noted that the negative effects were not entirely due to released Cu^{2+} ions from the dissolution of CuO particles. In a six-day petri dish study, radish and ryegrass were exposed to bulk and NP CuO NP, as well as Cu^{2+} ions, and the authors reported significant reductions in the root and shoot growth at 10–1000 mg/L (Atha et al., 2012). The observed toxicity was equivalent when the NP and ion were used at the same nominal concentration. However, when comparing the NP exposure to the ion dose that corresponded to the actual dissolution from the particles, the inhibition in the root and shoot growth was significantly higher in the NP exposure. Other studies with cilantro (*Coriandrum sativum*) have demonstrated a significant reduction in shoot mass upon exposure to CuO NPs and micro-copper (μCuO) (Zuverza-Mena et al., 2015). Similarly, wheat (*Triticum aestivum*) grown in a sand matrix with 500 mg/kg CuO NPs was significantly reduced. Here, authors attributed the phytotoxicity to dissolved Cu from CuO NPs (Dimkpa et al., 2012). In the current study, CuO transformed in the soil to ionic forms during the weathering process, with subsequent transformation to reduced forms of the element. The relationship between the time course of these transformations and potential toxicity to the growing plant is currently not known. However, our findings taken with that of the current literature clearly suggest that irrespective of the medium, the phytotoxicity of CuO NPs is not entirely due to the released Cu^{2+} ions. This is in agreement with our molecular studies, where the expression level of genes involved in Cu transport and detoxification (U and W) was assessed (SI Figure S5). Our results showed that NPs and bulk (W and U) treatments have similar expression profiles and showed a general modest down-regulation of all genes analyzed. Conversely, when compared to

ion treatments at 10% of the NP/bulk nominal dose, a much stronger up-regulation of genes was noted. These results suggest that although NPs and bulk treatments might be dissolving and releasing ions, the amount is not enough to trigger selected transport genes and not solely responsible for observed Cu accumulation and toxicity.

Co-contaminant exposure effects on the pesticide content in L. sativa

Chlordane was only detected in lettuce root tissues. In previous studies we have shown measurable chlordane in lettuce shoots (Hamdi et al., 2015; Mattina et al., 2000) but this discrepancy is likely due to differences in experimental design. Hamdi et al. (2015) exposed plants to freshly prepared chlordane solution in vermiculate, whereas the current study involved field incurred residues originating from a 1968 pesticide application (Mattina et al., 2000). With regard to Mattina et al. (2000), the plants in that study were grown in the field under full life cycle conditions, whereas those in the current study involved a shorter growth period under more narrow conditions. The non-detection of chlordane across the unexposed control and treatment samples does demonstrate that none of the Cu exposures significantly impacted the translocation of chlordane to the shoots. Furthermore, no correlation was found between Cu content and pesticides in plant root tissues. However, in the unweathered exposure, NP and ionic Cu did suppress total chlordane uptake relative to bulk and unexposed controls. Interestingly, this difference disappeared with weathering. Interestingly, with regard to chlordane uptake, the bulk and NP exposures seemed to respond differently to weathering (SI Figure S6). In the bulk treatment, total chlordane amounts are reduced by half with weathering; for the NP exposure, the levels are equivalent across the weathering period. This is particularly interesting given the above mentioned synchrotron data showing that Cu species in U and W treatment were different. Studies focusing on NP co-contaminant effect on plant in terrestrial systems are rather limited. De la Torre-Roche et al. (2013b) reported that silver (Ag) NP exposure significantly decreased the accumulation of DDE by zucchini and soybean. Similarly, multi-wall carbon nanotubes decreased the uptake of weathered DDE and chlordane in four agricultural crops, likely due to the nanomaterials high absorption capabilities for hydrophobic residues (De la Torre-Roche et al., 2013a). Conversely, fullerenes appeared to increase or cause no effect upon the uptake of organic compounds by plants (De la Torre-Roche et al., 2013a; Ma & Wang, 2010). The mechanisms controlling the interaction of engineered NPs with coexisting organic and inorganic contaminants, as well as the significance of these processes to exposed receptors, remain largely unknown.

Conclusions

This study highlights that NPs trophic transfer is dependent on particle type, exposure conditions, and producer/consumer species. Notably, exposure to 400 mg/kg bulk or NP CuO, or to 40 mg/kg ionic Cu, resulted in little toxicity to lettuce and no measurable trophic transfer to insect or lizard species, regardless of exposure type. Our findings do suggest that weathering conditions may result in transformation (dissolution, reduction, sulfidation) processes that significantly influence NP availability to plants. Importantly, the μ-XRF analysis also demonstrated altered Ca and Cu distribution within the plants upon weathering; the implications of these effects on overall nutritional quality are not known. Our molecular studies suggest that although NPs are clearly dissolving (required prior to the reductive transformations noted above) in soil, the released ionic concentration of Cu ion is insufficient to trigger the response from plants exposed to 10 times less Cu in ionic form. This also raises questions over what form the Cu accumulated by NP-exposed plants is actually in. In natural systems, it is probable that NPs interactions with co-contaminants in soil (e.g. pesticides, heavy metals) will occur, which could have an indirect effect on plants. Our studies suggest that the particle-size specific speciation changes that occur with NPs in soil may significantly affect pesticide availability to plants. Lastly, this study clearly demonstrates the complexity of NP interactions that must be characterized in order to accurately assess exposure and predict the risk.

Acknowledgements

We thank USDA-AFRI (#2011-67006-30181) for funding. LP acknowledges support of project "BIOMAN" funded by Fondazione CARIPLO. LP acknowledges University of Parma Research Fellowship n. 3BIOS/2014 entitled "Analisi sulla sicurezza per la salute e per l'ambiente determinata dalle interazioni tra nanoparticelle, nanomateriali e piante di interesse agroalimentare". OPD acknowledges a sub-award (#S14000000000026) from CAES to UMass Amherst.

Disclosure statement

The authors report no conflicts of interest.

Funding

We thank USDA-AFRI (#2011-67006-30181) for funding. LP acknowledges support of project "BIOMAN" funded by Fondazione CARIPLO.

References

Anjum NA, Adam V, Kizek R, Duarte AC, Pereira E, Iqbal M, et al. 2015. Nanoscale copper in the soil–plant system – toxicity and underlying potential mechanisms. Environ Res 138:306–25.

Atha DH, Wang H, Petersen EJ, Cleveland D, Holbrook RD, Jaruga P, et al. 2012. Copper oxide nanoparticle mediated DNA damage in terrestrial plant models. Environ Sci Technol 46:1819–27.

Boutigny S, Sautron E, Finazzi G, Rivasseau C, Frelet-Barrand A, Pilon M, et al. 2014. HMA1 and PAA1, two chloroplast-envelope PIB-ATPases, play distinct roles in chloroplast copper homeostasis. J Exp Bot 65:1529–40.

Da Costa MVJ, Sharma PK. 2016. Effect of copper oxide nanoparticles on growth, morphology, photosynthesis, and antioxidant response in *Oryza sativa*. Photosynthetica 54:110–19.

De la Torre R, Servin A, Hawthorne J, Xing B, Newman LA, Xingmao M, et al. 2015. Terrestrial trophic transfer of bulk and nanoparticle La_2O_3 does not depend on particle size. Environ Sci Technol 49:11866–74.

De La Torre-Roche R, Hawthorne J, Deng Y, Xing B, Cai W, Newman LA, et al. 2013. Multiwalled carbon nanotubes and C60 fullerenes differentially impact the accumulation of weathered pesticides in four agricultural plants. Environ Sci Technol 47:12539–47.

De La Torre-Roche R, Hawthorne J, Musante C, Xing B, Newman LA, Ma X, White JC. 2013b. Impact of Ag nanoparticle exposure on p,p′-DDE bioaccumulation by *Cucurbita pepo* (Zucchini) and *Glycine max* (Soybean). Environ Sci Technol 47:718–25.

del Pozo T, Cambiazo V, González M. 2010. Gene expression profiling analysis of copper homeostasis in *Arabidopsis thaliana*. Biochem Biophys Res Commun 393:248–52.

Dimkpa CO, McLean JE, Latta DE, Manangon E, Britt DW, Johnson WP. 2012. CuO and ZnO nanoparticles: phytotoxicity, metal speciation, and induction of oxidative stress in sand-grown wheat. J Nanopart Res 14:1125.

Dimkpa CO, McLean JE, Martineau N, Britt DW, Haverkamp R, Anderson AJ. 2013. Silver nanoparticles disrupt wheat (*Triticum aestivum* L.) growth in a sand matrix. Environ Sci Technol 47:1082–90.

Evans P, Matsunaga H, Kiguchi M. 2008. Large-scale application of nanotechnology for wood protection. Nat Nanotechnol 3:577.

Fernandes JC, Henriques FS. 1991. Biochemical, physiological, and structural effects of excess copper in plants. Bot Rev 57:246–73.

Ginocchio R, Rodriguez PH, Badilla-Ohlbaum R, Allen HE, Lagos GE. 2002. Effect of soil copper content and pH on copper uptake of selected vegetables grown under controlled conditions. Environ Toxicol Chem 21:1736–44.

Grotz N, Guerinot ML. 2006. Molecular aspects of Cu, Fe and Zn homeostasis in plants. Biochim Biophys Acta 1763:595–608.

Hamdi H, De La Torre-Roche R, Hawthorne J, White JC. 2015. Impact of non-functionalized and amino functionalized multiwall carbon nanotubes on pesticide uptake by lettuce (*Lactuca sativa* L.). Nanotoxicology 9:172–80.

Hawthorne J, De la Torre Roche R, Xing B, Newman LA, Ma X, Majumdar S, et al. 2014. Particle-size dependent accumulation and trophic transfer of cerium oxide through a terrestrial food chain. Environ Sci Technol 48:13102–9.

Himelblau E, Amasino RM. 2000. Delivering copper within plant cells. Curr Opin Plant Biol 3:205–10.

Holbrook DR, Murphy KE, Morrow JB, Cole KD. 2008. Trophic transfer of nanoparticles in a simplified invertebrate food web. Nat Nanotechnol 3:352–5.

Hong J, Rico C, Zhao L, Adeleye AS, Keller AA, Peralta-Videa JR, Gardea-Torresdey JL. 2015. Toxic effects of copper-based nanoparticles or compounds to lettuce (*Lactuca sativa*) and alfalfa (*Medicago sativa*). Environ Sci Process Impacts 17:177–85.

Hoops D. 2015. A perfusion protocol for lizards, including a method for brain removal. MethodsX 2:165–73.

Isleyen M, Sevim P, Hawthorne J, Berger W, White JC. 2013. Inheritance profile of weathered chlordane and p,p′-DDTs accumulation by *Cucurbita pepo* hybrids. Int J Phytoremediat 15:861–76.

Judy J, Unrine JM, Bertsch PM. 2011. Evidence for biomagnification of gold nanoparticles within a terrestrial food chain. Environ Sci Technol 45:776–81.

Keller AA, Lazareva A. 2014. Predicted releases of engineered nanomaterials: from global to regional to local. Environ Sci Technol Lett 1:65–70.

Kim S, Lee S, Lee I. 2012. Alteration of phytotoxicity and oxidant stress potential by metal oxide nanoparticles in *Cucumis sativus*. Water Air Soil Pollut 223:2799–806.

Larue C, Castillo-Michel H, Stein RJ, Fayard B, Pouyet E, Villanova J, et al. 2016. Innovative combination of spectroscopic techniques to reveal nanoparticle fate in a crop plant. Spectrochim Acta B 119:17–24.

Le Van N, Ma C, Shang J, Rui Y, Liu S, Xing B. 2016a. Effects of CuO nanoparticles on insecticidal activity and phytotoxicity in conventional and transgenic cotton. Chemosphere 144:661–70.

Le Van N, Rui Y, Cao W, Shang J, Liu S, Quang TN, Liu L. 2016b. Toxicity and bio-effects of CuO nanoparticles on transgenic Iptcotton. J Plant Interact 11:108–16.

Levard C, Reinsch BC, Michel FM, Oumahi C, Lowry GV, Brown GE. 2011. Sulfidation processes of PVP-coated silver nanoparticles in aqueous solution: impact on dissolution rate. Environ Sci Technol 45:5260–6.

Liu J, Sonshine DA, Shervani S, Hurt RH. 2010. Controlled release of biologically active silver from nanosilver surfaces. ACS Nano 4:6903–13.

Lopez-Bucio J, Nieto-Jacobo MF, Ramirez-Rodriguez V, Herrera-Estrella L. 2000. Organic acid metabolism in plants: from adaptive physiology to transgenic varieties for cultivation in extreme soils. Plant Sci 160:1–13.

Ma X, Wang C. 2010. Fullerene nanoparticles affect the fate and uptake of trichloroethylene in phytoremediation systems. Environ Eng Sci 27:989–92.

Majumdar S, Trujillo-Reyes J, Hernandez-Viezcas JA, White JC, Peralta-Videa JR, Gardea-Torresdey JL. 2016. Cerium biomagnification in a terrestrial food chain: influence of particle size and growth stage. Environ Sci Technol 50:6782–92.

Mattina MJI, Iannucci-Berger W, Dykas L. 2000. Chlordane uptake and its translocation in food crops. J Agric Food Chem 48:1909–15.

Mudunkotuwa I, Pettibone JM, Grassian VH. 2012. Environmental implications of nanoparticle aging in the processing and fate of copper-based nanomaterials. Environ Sci Technol 46:7001–10.

Musante C, White JC. 2012. Toxicity of silver and copper to *Curcurbita pepo*: differential effects of nano and bulk-size particles. Environ Toxicol 9:510–17.

Nair PMG, Chung IM. 2014. Impact of copper oxide nanoparticles exposure on *Arabidopsis thaliana* growth, root system development, root lignification, and molecular level changes. Environ Sci Pollut Res 21:12709–22.

Nair PMG, Chung IM. 2015. The responses of germinating seedlings of green peas to copper oxide nanoparticles. Biolog Plantarum 59:591–5.

Nair PMG, Kim S, Chung IM. 2014. Copper oxide nanoparticle toxicity in mung bean (*Vigna radiata* L.) seedlings: physiological and molecular level responses of in vitro grown plants. Acta Physiol Plant 36:2947–58.

Pagano L, Servin AD, De la Torre-Roche R, Mukherjee A, Majumdar S, Hawthorne J, et al. 2016. Molecular response of crop plants to engineered nanomaterials. Environ Sci Technol 50:7198–207.

Perreault F, Oukarroum A, Pirastru L, Sirois L, Gerson Matias W, Popovic R. 2010. Evaluation of copper oxide nanoparticles toxicity using chlorophyll *a* fluorescence imaging in *Lemna gibba*. J Bot 2010:763142.

Pradhan S, Patra P, Mitra S, Kumar Dey K, Basu S, Chandra S, et al. 2015. Copper nanoparticle (CuNP) nanochain arrays with a reduced toxicity response: a biophysical and biochemical outlook on *Vigna radiata*. J Agric Food Chem 63:2606–17.

Romero-Freire A, Lofts S, Martin Peinado FJ, van Gestel CAM. 2017. Effects of aging and soil properties on zinc oxide nanoparticle availability and its ecotoxicological effects to the earthworm *Eisenia andrei*. Environ Toxicol Chem 36:137–46.

Sajid M, Ilyas M, Basheer C, Tariq M, Daud M, Baig N, Shehzad F. 2015. Impact of nanoparticles on human and environment: review of toxicity factors, exposures, control strategies, and future prospects. Environ Sci Pollut Res Int 22:4122.

Scheckel KG, Luxton TP, El Badawy AM, Impellitteria CA, Tolaymat TM. 2010. Synchrotron speciation of silver and zinc oxide nanoparticles aged in a kaolin suspension. Environ Sci Technol 44:1307–12.

Seitz F, Luderwald S, Rosenfeldt RR, Schulz R, Bundschuh M. 2015. Aging of TiO_2 nanoparticles transiently increases their toxicity

to the pelagic microcrustacean *Daphnia magna*. PLoS One 10:e0126021.

Servin AD, De la Torre R, Castillo-Michel H, Pagano L, Hawthorne J, Musante C, et al. 2017. Exposure of agricultural crops to nanoparticle CeO_2 in biochar-amended soil. Plant Physiol Biochem 110:147–57.

Servin AD, Elmer W, Mukherjee A, De la Torre-Roche R, Hamdi H, White JC, et al. 2015. A review of the use of engineered nanomaterials to suppress plant disease and enhance crop yield. J Nanopart Res 17:92.

Servin AD, White JC. 2016. Nanotechnology in agriculture: next steps for understanding engineered nanoparticle exposure and risk. Nanoimpact 1:9–12.

Shaw AK, Ghosh S, Kalaji HM, Bosa K, Brestic M, Zivcak M, Hossain Z. 2014. Nano-CuO stress induced modulation of antioxidative defense and photosynthetic performance of Syrian barley (*Hordeum vulgare* L.). Environ Exp Bot 102:37–47.

Shaw AK, Hossain Z. 2013. Impact of nano-CuO stress on rice (*Oryza sativa* L.) seedlings. Chemosphere 93:906–15.

Sole´ VA, Papillon E, Cotte M, Walter P, Susini JA. 2007. Multiplatform code for the analysis of energy-dispersive X-ray fluorescence spectra. Spectrochim Acta B 62:63–8.

Trujillo-Reyes J, Majumdar S, Botez CE, Peralta-Videa JR, Gardea-Torresdey JL. 2014. Exposure studies of core-shell Fe/Fe_3O_4 and Cu/CuO NPs to lettuce (*Lactuca sativa*) plants: are they a potential physiological and nutritional hazard? J Hazard Mater 267:255–63.

Unrine JM, Shoults-Wilson WA, Zhurbich O, Bertsch PM, Tsyusko OV. 2012. Trophic transfer of Au nanoparticles from soil along a simulated terrestrial food chain. Environ Sci Technol 46:9753–60.

Wang Z, Von Dem Bussche A, Kabadi PK, Kane AG, Hurt RH. 2013. Biological and environmental transformations of copper-based nanomaterials. ACS Nano 7:8715–27.

Wang Z, Xie X, Zhao J, Liu X, Feng W, White JC. 2012. Xylem- and phloem-based transport of CuO nanoparticles in maize (*Zea mays* L.). Environ Sci Technol 46:4434–41.

White P, Broadley MR. 2003. Calcium in plants. Ann Bot 92:487–511.

Zhao L, Sun Y, Hernandez-Viezcas JA, Hong J, Majumdar S, Niu G, et al. 2015. Monitoring the environmental effects of CeO_2 and ZnO nanoparticles through the life cycle of corn (*Zea mays*) plants and in situ μ-XRF mapping of nutrients in kernels. Environ Sci Technol 49:2921–8.

Zuverza-Mena N, Medina-Velo IA, Barrios AC, Tan W, Peralta-Videa JR, Gardea-Torresdey JL. 2015. Copper nanoparticles/compounds impact agronomic and physiological parameters in cilantro (*Coriandrum sativum*). Environ Sci Process Impacts 17:1783–93.